Structural and spectroscopic in vivo imaging of the human retina with scanning light ophthalmoscopy

Damodaran, M.

2020

document version
Publisher's PDF, also known as Version of record

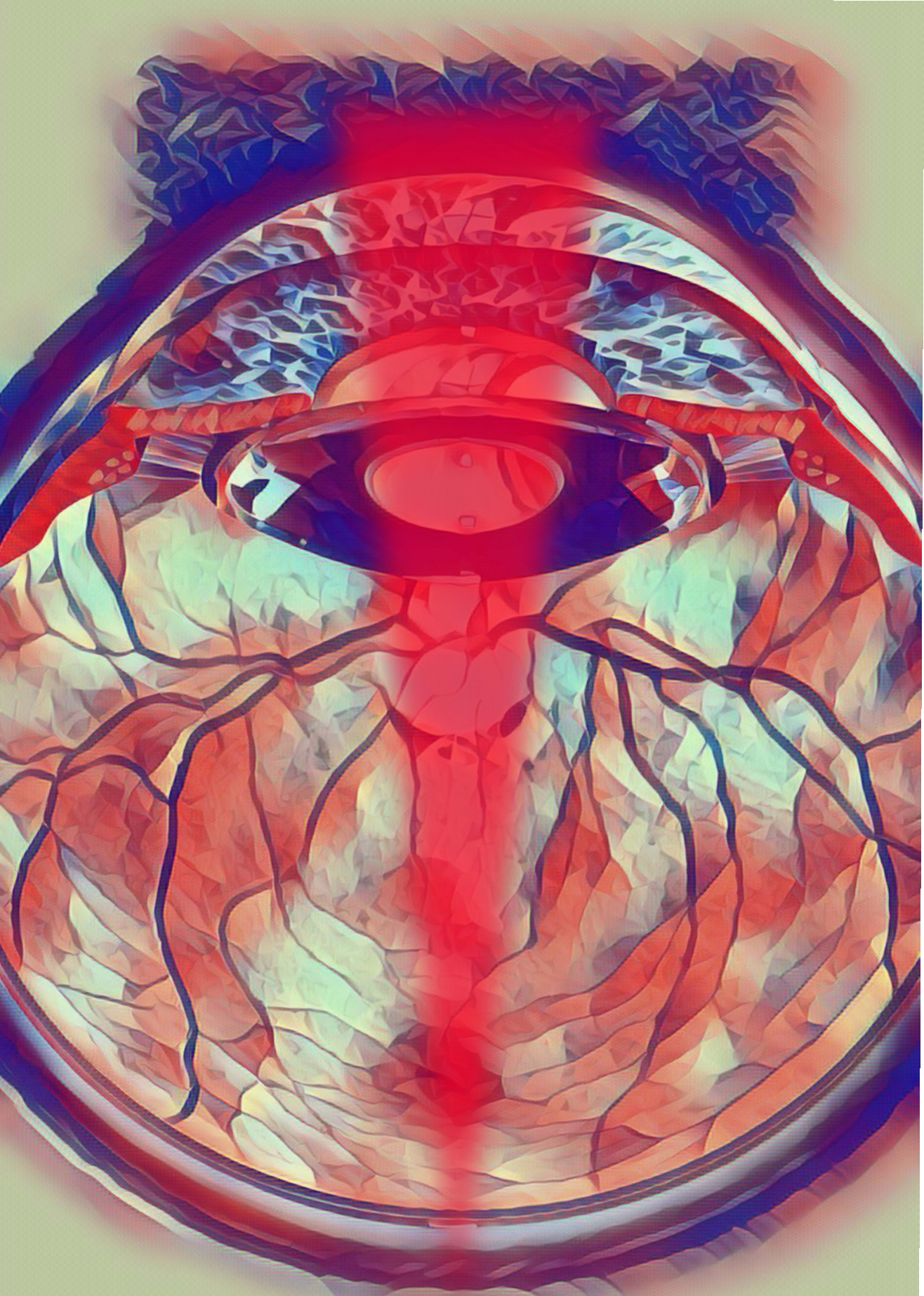

1

General introduction

Overview

The eye is an organ which gives us the sense of sight and allows us to observe the surrounding world. We use our eyes in almost every activity we perform and hence a disease which affects vision has a negative impact on a person's quality of life. Age-related diseases are a significant public health concern, especially in the western world where there is an increase in the median age of the population [1]. Particularly, retinal diseases can result in visual function impairment, which can lead to reduced social interactions, loss of independence and disability. According to the WHO, about 1.3 billion people live with some visual function impairment, of which 270 million people have moderate to severe vision impairment [2]. About 80 % of all vision impairments globally are considered avoidable. Retinal pathologies and injuries exhibit structural and functional changes in the retina and are assessed using ocular imaging techniques. Retinal imaging is thus vital for our understanding of retinal diseases, and effective clinical evaluation, follow-up and treatment.

Advancements in retinal imaging have drastically improved the quality of eye care in the past two decades. Nevertheless, the current clinical evaluation of retinal diseases relies considerably on subjective visualisation of the retinal anatomy. In many pathological conditions, however, better and more objective imaging and image analysis methods are required. New techniques that can establish a correlation between retinal diseases and optical properties need to be developed. The various optical properties of the retina can be correlated to diagnostic criteria to provide new means for improving clinical care in ophthalmology. For example, a quantitative *in vivo* characterisation of spectral properties of the retina helps in understanding the pathophysiology of various diseases [3]. This thesis focuses on two major approaches to retinal imaging which can improve clinical care in ophthalmology:

1. Structural imaging of the retina using a low-cost, compact, novel **digital micromirror based ophthalmoscope**
2. Quantitative, functional imaging of the retina using a **multispectral scanning laser ophthalmoscope**.

1.1 Human eye: anatomy and physiology

Advancements in retinal imaging have drastically improved the quality of eye care in the past two decades. However, the current clinical evaluation of retinal diseases relies considerably on subjective visualisation of the retinal anatomy. In many

pathological conditions, however, better and more objective imaging and image analysis methods are required. New The eye is an essential sensory organ which provides the ability to see in both bright and dim light, focusing on objects both near and far. The eye can detect three primary colours and transmit the information to the brain, which processes and perceives the image in millions of colours. A schematic cross-section of the eye and the retina is shown in Fig.1.1.

Cornea

About one-sixth of the anterior layer of the eye bulges and forms the transparent cornea, the aspherical bulge which serves as the outer transparent window of the eye. The cornea is made up of connective tissue with a thin layer of epithelium on the surface. The cornea contains hardly any cells and blood vessels and is transparent. Light enters the eye through the cornea, and the air-cornea interface does most of the focusing of the light. The cornea transmits about 99 % of visible light [4]. The cornea continues as **sclera**, the opaque portion of the eye. The sclera runs along the circumference of the eye and makes up the remaining posterior five-sixths of the eye's outer layer. The sclera is responsible for the protection of the vital inner layers of the eye and serves to attach the extra-ocular muscles, which aid in eye motion.

Iris, lens and humor

After the cornea, the light passes the anterior part of the eye through the **pupil**. The pupil is the central aperture in the iris and regulates the amount of light entering the eye. The **iris**, a pigmented disc, is visible in most eyes due to the transparency of the cornea. The iris is mostly made up of smooth muscle fibers and connective tissue. As the flux of light entering the eye reduces, the smooth muscles of the iris pull away from the centre, causing the pupil to dilate. On the other hand, if there is a sudden influx of light, the sphincter muscles in the iris pull toward the centre, causing the pupil to contract and allowing less light to reach the retina.

The transparent and crystalline **lens** of the eye is located behind the iris, suspended by ciliary muscles. When viewing an object at infinity, the ciliary muscles pull on the suspension ligaments causing the entire lens to flatten, enabling the lens to focus light from a far-away object. When the eye views an object at a near distance, ciliary muscles contract causing the suspension ligaments to relax. This action causes both lens surfaces to become more convex and enables the eye to focus nearby.

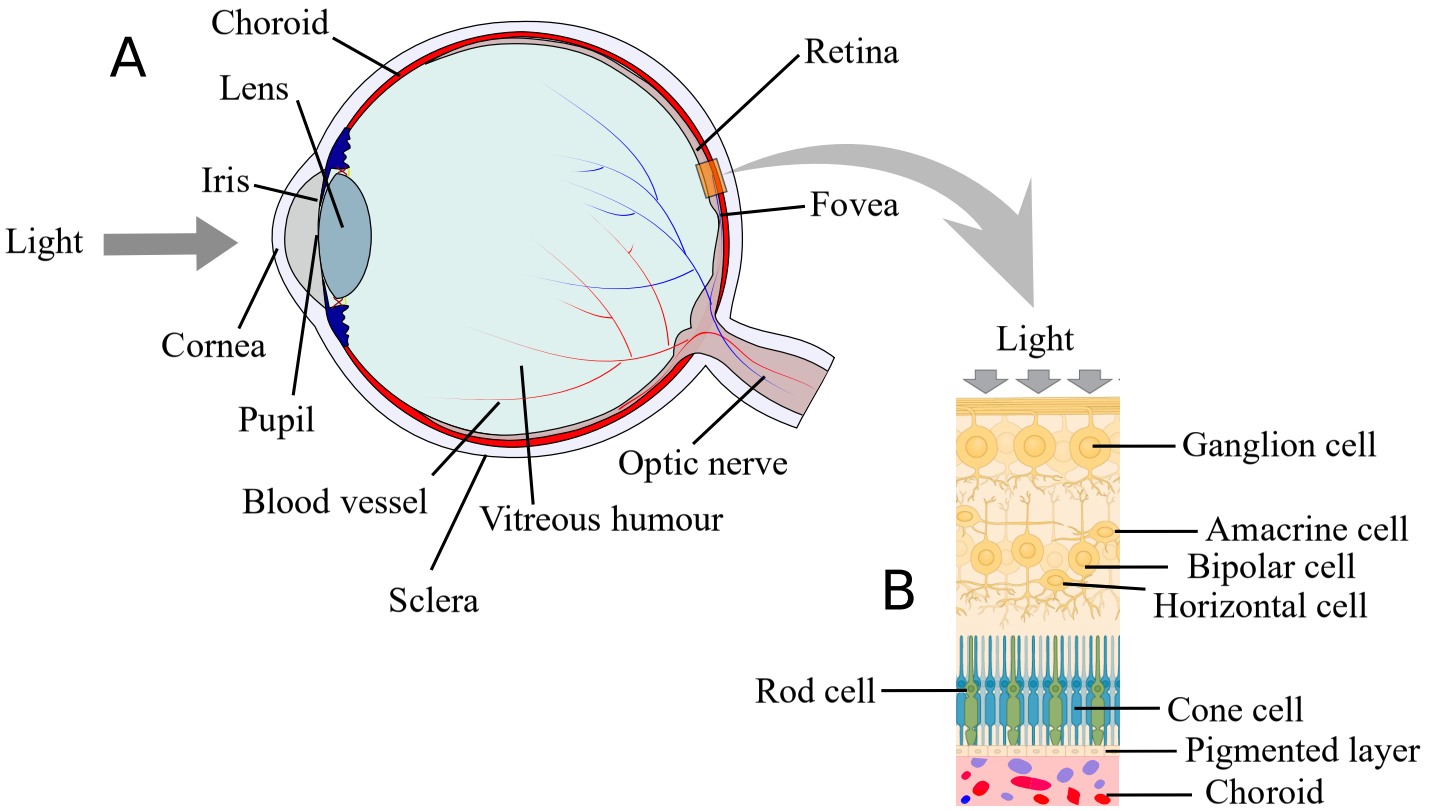

Figure 1.1: A: Cross-section of the human eye and its various constituents — The light enters the eye through the cornea and is focused on the retina by the lens. The blood vessels supply oxygen and nutrients to the retina. B: Cross-section of the retina showing different layers of cells, each performing a special function, [image adapted from Wikipedia]

The **vitreous humor** is a clear, transparent jelly-like substance which occupies the posterior part of the eye. It holds about 80% of the volume of the eyeball. The vitreous keeps the eye structurally intact.

Retina

The retina is a thin multi-layered tissue (Fig.1.1B) with an average thickness of 300 µm, which is responsible for the critical task of receiving light from the external world and transmitting visual stimuli to the brain. Various insults to this delicate structure can thus generate pathological processes and lead to retinal disease(s).

The retina consists of two components: an innermost layer of retinal pigment epithelium (RPE) which is composed of a single layer of melaninated cells, and the neural retina which is a multi-layered structure containing photoreceptors as well as neurons. These two components together are typically called the retina, and it is subdivided into nine recognisable layers: nerve fiber layer (**NFL**), ganglion cell layer (**GCL**), inner plexiform layer (**IPL**), inner nuclear layer (**INL**), outer plexiform layer (**OPL**), outer nuclear layer (**ONL**), external limiting membrane (**ELM**), photoreceptor layer (**PL**), and the retinal pigment epithelium (**RPE**). A histological cross-section of the human retina is shown in Fig. 1.2. The structure and function of each layer of the retina is a fascinating field in itself and is studied by many vision scientists. A brief description of each layer might help the reader in appreciating the complexity of the retina and the vital role it plays in vision.

The **NFL** is formed by the extension of the fibres of the optic nerve. It has the highest thickness near the optic disc and is made up of the support cells of the neural retina. NFL is a sensitive structure, and thus some process can start its spontaneous apoptosis. Any adverse situation can make some damage on NFL such as high intraocular pressure, inflammation, vascular disease and hypoxia [6].

The **IPL** is a region of the retina that is built up of a compact reticulum of fibrils arranged by interlaced dendrites of retinal ganglion cells. A retinal ganglion cell is a variety of neuron found in the **GCL** of the retina of the eye. It collects visual stimuli from photoreceptors through two intermediate cell types, namely bipolar cells and retinal amacrine cells [7].

The **INL** or layer of inner granules of the retina, is made up of several closely arranged cells, namely the bipolar cells, the horizontal cells, and the amacrine cells. The **OPL** is a layer of neuronal synapses in the retina. It consists of a compact network of synapses within dendrites of horizontal cells from the **INL**, and photoreceptor cell inner segments from the **ONL**. It is much thinner than the **IPL**, where amacrine cells synapse with retinal ganglion cells. The **ONL** is typical for verte-

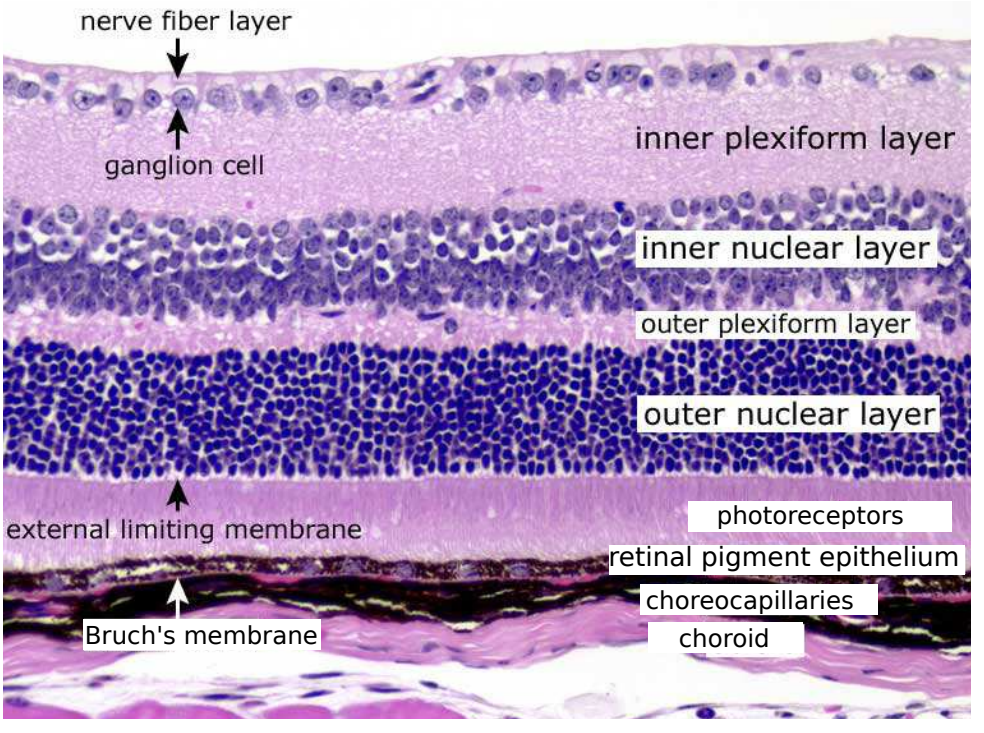

Figure 1.2: Histological cross-section of the posterior eye: retinal layers, choroid and sclera [5].

brate retina and is assumed to be the light-detecting portion of the eye. Like the **INL**, the **ONL** contains several strata of oval nuclear bodies [7].

The **PL** consists of the rod and cone cells. The light must cut across many layers before reaching the rods and cones. Rod cells are cylindrical, while the cone cells have conical outer segments. The rod cells are more receptive to the light stimuli and thus are primarily used in low light levels. The resulting image from the rod cells is monochromatic. The cone cells are sensitive to distinct wavelengths of light and allow the perception of colours and complete visible information. The photoreceptor layer is devoid of any blood capillaries [8].

The outermost layer closest to the choroid is the **RPE** which contains a single sheet of cuboid pigmented cells, with perform the function of absorbing light and thus preventing stray light from reflecting onto the rods and cones. Compact and tight interfaces between the cells in this layer establish the so-called 'blood-retina barrier' to regulate and balance the exchange of molecules from the blood to the retina and vice-versa. The RPE cells play an essential role in nourishing the overlying outer retina. They facilitate the diffusion of nutrients from the choroid. **Bruch's**

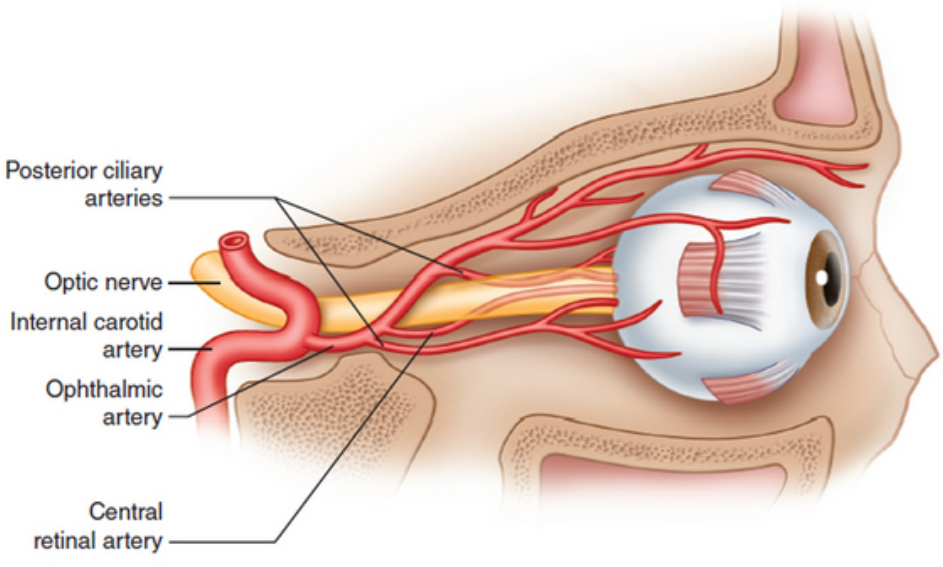

Figure 1.3: Blood supply to the eye: The ophthalmic artery is a branch of the internal carotid artery and divides into the central retinal artery and the posterior ciliary arteries. The former supplies blood to the outer layers of the retina while the later supplies blood to the choroid. Image adapted from Ichsan *et al.* [12].

membrane is the innermost layer of the choroid.

The axons from all the retinal ganglion cells converge and leave the eye through the optic nerve. The point where it exits is the **optic disc** or **optic nerve head (ONH)**. This area is incapable of detecting light, as this point is by definition, a break in the retina. Therefore the ONH creates a blind spot in the lateral visual field. The **fovea** is a small depression in the central portion of the retina. The inner layers of the retina are drastically reduced (or absent) in the fovea. The dominant layer of the fovea is the photoreceptor layer composed exclusively of cone cells. These cells are also slender than they are elsewhere in the retina to accommodate their dense packing. There is a 1:1 ratio of ganglion cells to photoreceptors in the fovea to facilitate excellent discrimination of colours and details. Blood vessels are also absent in the foveal region to allow light to pass unimpeded to the photoreceptors. The fovea is an avascular zone.

1.1.1 Blood supply to the retina

One of the main objectives of the thesis is measuring the blood oxygenation in the retinal vessels. Therefore it is important to understand how the blood is supplied to the retina. The blood supply of the entire eye comes from the ophthalmic artery,

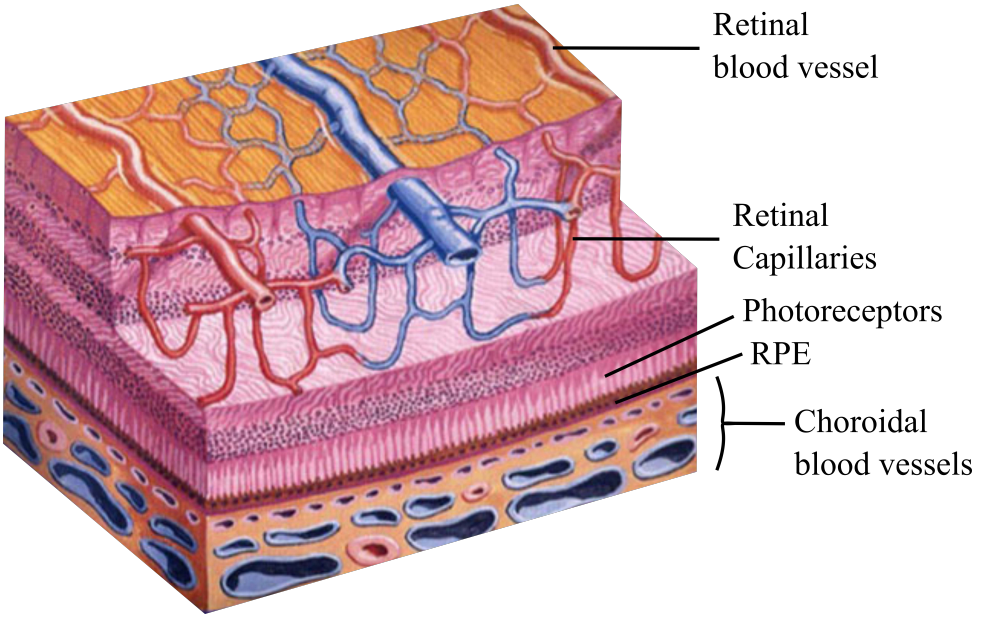

Figure 1.4: Retinal layers and blood vessels: The top layers are supplied oxygen through the retinal vasculature while choroidal vasculture supplies oxygen to the bottom layers (image courtesy of Novartis)

which is a branch of the internal carotid artery, as shown in Fig. 1.3. The retinal circulation originates from the central retinal artery (CRA), which is a branch of the ophthalmic artery [9]. The CRA travels inside the optic nerve and reaches the retina to branch from arteries to arterioles and capillaries into deeper layers, as shown in Fig. 1.4. The capillaries are organised mainly in two different layers, one in the NFL and another in the inner nuclear layer. The retinal capillaries continue to venules, which merge to form the central retinal vein (CRV) and leave the eye through the optic nerve [10, 11].

The choroidal circulation originates from the posterior ciliary arteries. The choroidal vessels can be divided (from outside to inside) into a layer of large arteries; a layer of medium-sized arteries and arterioles ; an innermost layer of choriocapillaris. In healthy eyes, the choroid does not penetrate the retina and does therefore not obscure vision. Oxygen diffuses from the choriocapillaris, through the retinal pigment epithelium to reach the photoreceptors which have high oxygen demand and high metabolic rate. The concentration gradient drives the diffusion of oxygen from the choriocapillaris to the photoreceptors [13].

The retinal and choroidal vasculatures are different in many ways. The retinal vasculature is sparse as a dense network can obscure vision. On the other hand,

Figure 1.5: Common retinal pathologies and functional changes — Retinal pathology affects vision and reduces the quality of life. The simulated images show the effect of visual impairments [20]

the choroidal vasculature is dense as there is no scope to obscure vision. The retinal circulation penetrates the retinal tissue, and this decreases diffusion distances from capillaries to retinal cells.

1.1.2 Common retinal pathologies

As explained in the previous section, the retina is an incredibly intricate structure, hence is prone to many retinal pathologies due to impairment or injury to one or some of its components. The capacity of the retinal tissue to respond to such damages depends mainly on: the specific cells and tissue involved, type, duration and severity of the injury. The broad range of retinal conditions that may exist is too extensive to review in this brief chapter. Instead, we discuss a few important retinal diseases.

Age related macular degeneration (AMD) is a disease that causes blindness, and is the most common disease that causes blindness in industrialised countries [14]. AMD is also the most common condition whose incidence increases with ageing. The dry form of AMD is identified by drusen and extracellular deposits which accumulate beneath the RPE, and a loss of photoreceptors. In wet AMD, abnormal blood vessels grow under the retina and macula due to a process called choroidal neovascularization. These blood vessels may then leak and bleed, causing the macular region of the retina to bulge, destroying vision in the process. Vision loss due

to AMD may be rapid and severe.

Diabetic retinopathy (DR) occurs as small aneurysms or haemorrhages in the retinal tissue. When diabetes is uncontrolled, it damages blood vessels throughout the body. Diabetes results in reduced maintenance of the blood sugar levels, and in the long run, it affects the capillaries throughout the body. A particular example of the location in the body where tiny capillaries are affected is in the retina, resulting in DR.

Retinal vessel occlusions (RVO) is a retinal pathology which disturbs retinal blood flow and oxygenation. Occlusions can be broadly divided into vein occlusions and artery occlusions. Occlusions can be further divided into central occlusions, affecting the central retinal vein or artery, and branch occlusions, affecting branches of the central vessels. The primary symptom of retinal vascular occlusion is a sudden change in vision. This could include blurry vision or a partial or complete loss of sight.

Glaucoma is characterised by degeneration of the NFL and the optic nerve. In cases it is accompanied by loss of vision. Glaucoma has been traditionally linked to high intraocular pressure, although it is not necessarily associate with high pressure and several glaucoma patients have normal or low intraocular pressure [15]. But elevated intraocular pressure is a risk factor for glaucoma and lowering of the intraocular pressure is a widely accepted treatment for glaucoma. Reducing the intraocular pressure generally slows the progression of glaucoma, even in patients with low pressure. However, retinal blood flow does not follow changes in intraocular pressure linearly.

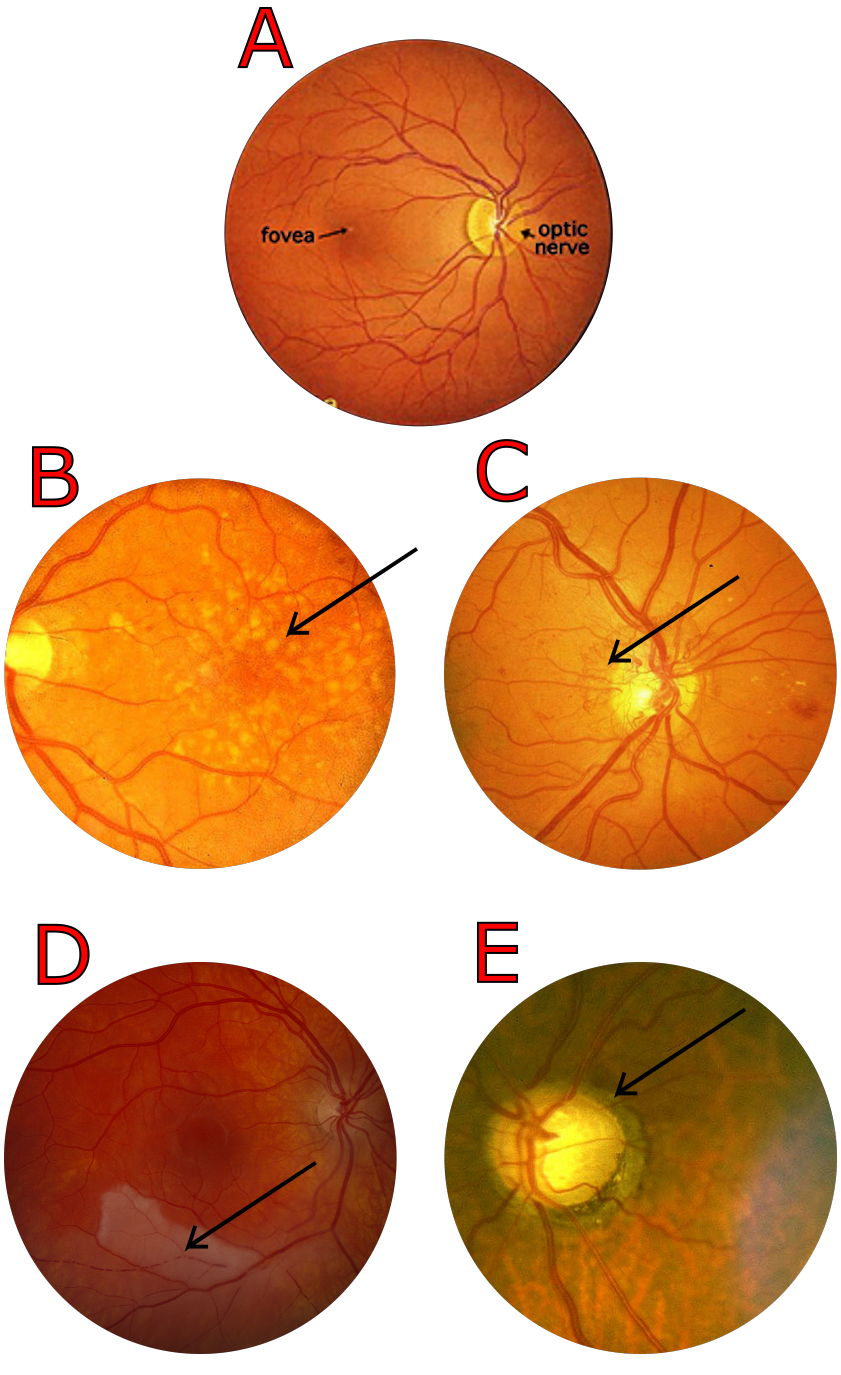

Figure 1.6: Common retinal pathologies and structural changes—A: Fundus image of a normal healthy human retina showing the optic nerve head and the fovea. B: Image of an eye with AMD. The arrow indicates drusen in the fundus [16]. C: Image of an eye with DR [17]. The arrow indicates the abnormal growth of blood vessels. D: image of an eye with RVO with the arrow showing blocked blood vessels in the retina [18]. E: an image of an eye with Glaucoma with the arrow showing the abnormal size of the ONH [19].

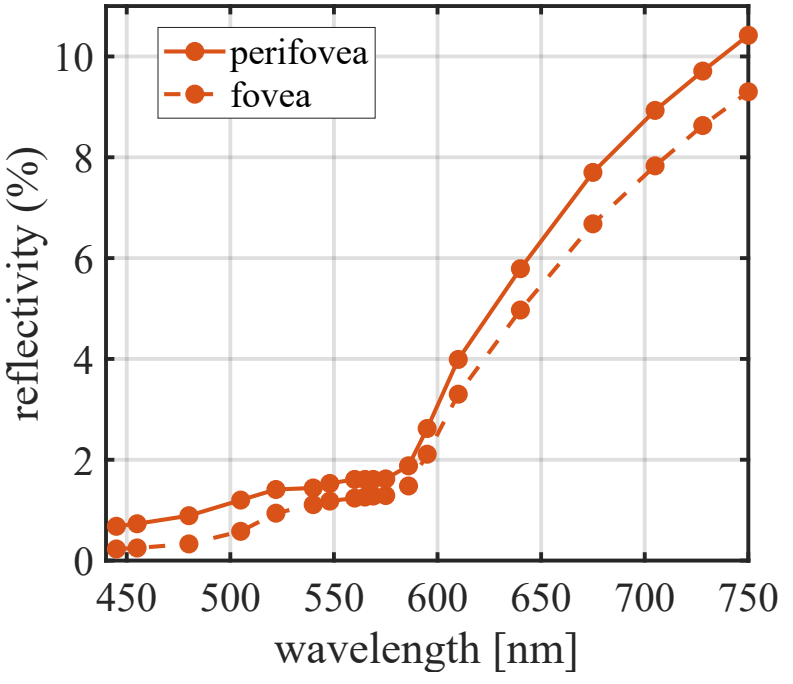

Figure 1.7: Reflection spectrum of the human retina in *perifoveal* and *foveal* region observed from 30 different human subjects. Data taken from Delori *et al.*[22].

1.2 Retinal imaging techniques

Non-invasive imaging of the retina presents some unique challenges because of its location in the posterior eye. The retina must be illuminated and imaged at the same time, a method which requires illumination and detection modules to share a common optical path. The retina is a low reflective [21, 22] (Fig. 1.7) and moderately scattering [23] surface. These attributes result in only a small fraction of the light illuminating the retina to reach the detector. Imaging the retina requires the optics of the eye to be used as a part of the imaging system. The optics of the cornea and the crystalline lens introduce aberrations in an imaging system.

Historical perspective

The invention of the ophthalmoscope by Helmholtz in 1851 [24] was the first breakthrough in modern imaging techniques (1.8A), especially towards the goal of imaging the retina. Helmholtz's design consisted of a partially reflecting mirror that directed light from a source onto the retina. In 1886, Jackman and Webster recorded

the first in-vivo human retinal photograph, showing the optic disc and larger blood vessels [25]. In the century that followed, fundus photography to document ophthalmoscopic findings progressed and became a necessary method for the examination and assessment of retinal disease. In 1961, the first successful fluorescein angiography was recorded in humans [26]. Fluorescein angiography has become the main diagnostic tool for the study of retinal flow.

The invention of the scanning laser ophthalmoscope (SLO) in the early 1980s [27–29] thrust the field of fundus imaging into a new era. Instead of capturing the image as a whole, SLO samples the retina point by point in a raster-like fashion with its laser beam. The SLO was combined with confocal optics in 1987 [30]. Despite fundus imaging and fluorescein angiography [31] being gold standards in ophthalmic clinical care, there are limitations of these techniques. These techniques give a macroscopic view of the retina and have a restricted ability for analysing the three-dimensional composition of the tissue. The retina is a three-dimensional structure, and microscopic visualisation of retinal features is possible only with good axial and transverse resolution. With this in mind, various new retinal imaging techniques have emerged to investigate the structure and function of the retina in great detail. For example, ultrasound has been used for eye diagnosis. The optical analogue, called Optical coherence tomography (OCT) was found in 1991 by Huang *et al*. [32] and transformed ophthalmic imaging. OCT uses low-coherence light with interferometry. Low coherence interferometry had been used previously to measure axial distances in the eye [33, 34]. The retina is virtually transparent with extremely low optical backscattering, but the great sensitivity of OCT allows detection of such weak signals. In contrast to conventional microscopy. A brief description of various retinal imaging modalities is given in this chapter, with in-depth working principles described in the next chapter.

1.2.1 Fundus photography

A fundus camera is used to take a snapshot image of the retina and typically has a wide field of view. A simple version of the fundus camera consists of an imaging system, illumination system, and usually also a fixation target. All of these systems must share common optics. Broadband flood illumination is used to illuminate the retina after enlarging the pupil of the eye using mydriating eye drops. The reflected and scattered light is captured by an area sensor such as a CCD camera. Almost every ophthalmic clinic in the world uses a fundus camera for retinal imaging. Fluorescein angiography can also be achieved using fundus camera-based techniques but with an intravenous injection of a fluorescent dye.

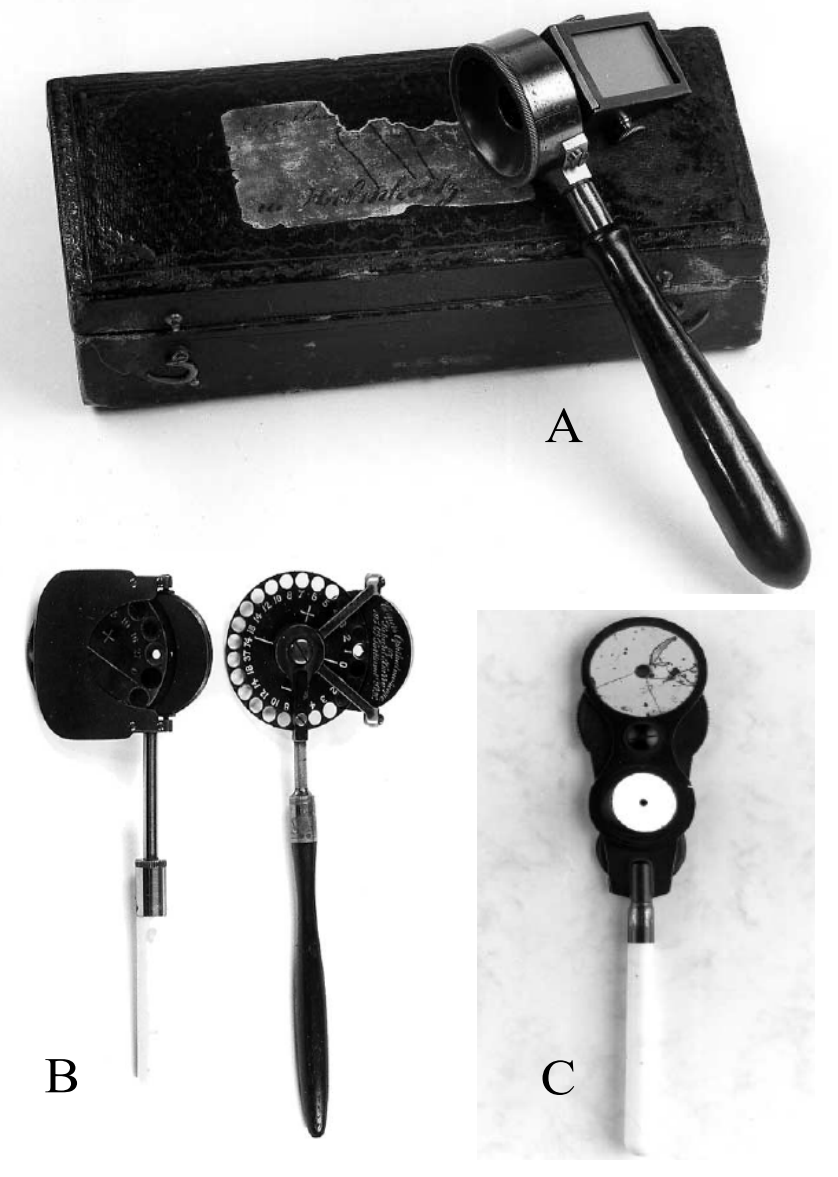

Figure 1.8: A: Early model of the Helmholtz ophthalmoscope (1851). B: John Coupers first ophthalmoscope, with a slide-in Rekoss disc behind a tilting mirror (left), Right: second model. C: Lindsay Johnson ophthalmoscope with two mirrors for direct and indirect ophthalmoscopy.

Fundus photography gives the necessary information to diagnose some retinal disease. The cost of fundus photography continues to be significantly lower than the newer techniques based on retinal scanning. Its main advantages are the easy interpretation, full colour, better detection of haemorrhages etc. Disadvantages in-

clude lack of quantitative description and hence inter-observer variability, the need of high photographic quality, and difficult serial comparison because of limited ability to detect subtle changes with a photograph. Another drawback of fundus photography is the need for high light intensity for illumination of the retina, on the order of 10-100 % of the maximum permissible levels [31], typically delivered by a flash.

1.2.2 Scanning Laser Ophthalmoscope

A scanning laser ophthalmoscope (SLO) produces retinal images by scanning a laser spot (line) and detecting backscattered light using a point (line) detector. High contrast images are achieved if a confocal pinhole [30] is used as it enables suppression of the scattered light, and thereby minimising the optical cross-talk outside a volume surrounding the focal point on the retina. SLO systems are used in clinics throughout the world and have been modified for different clinical applications. The diagnostic applications of SLO include detection of the structural biomarkers of AMD, Glaucoma, RVO and DR [35, 36]. SLOs have been combined with optical coherence tomography-based techniques (which are explained below) for eye motion tracking [37–40] as well as for optimal classification of diseases [41–44]. Furthermore, adaptive optics has been implemented in an SLO system with the help of a wavefront detection sensor, and this has enabled visualisation of rod and cone cells in the photoreceptor layer of the retina [45–47]. A detailed description of the working of an SLO is given in chapter 2.

1.2.3 Optical Coherence Tomography

As explained in section 1.1, the complicated structure of the retina demands precise visualization of pathology. OCT enables non-invasive, high-resolution imaging of the retina *in vivo*. OCT's axial resolution surpasses that of ultrasound or confocal SLO and resembles that of conventional histology[48, 49]. In OCT, the axial resolution is mainly determined by the bandwidth and wavelength of the optical source and therefore, the retina of the human eye can be imaged with at least 100 times better axial resolution [50]. Advancements in the field of OCT have led to the development of spectral-domain OCT [51–53]. In principle, an OCT operates as a low coherence Michelson interferometer. Interference occurs when the optical path difference between the sample and reference arms is within the coherence length of the source. As the source becomes less coherent, the coherence length shrinks, making the maximum optical path difference between reference and sample arms

needed for the interference to occur smaller.

1.3 Thesis aim and outline

Ophthalmic imaging has been an active area of clinical investigation that has been expanding steadily, providing scientists and doctors with valuable information. New diagnostic and therapeutic methods have been established in this field, driven by an overall need to advance clinical care in ophthalmology. New scanning and imaging technologies have had a significant impact on ophthalmology. Structural imaging techniques help in visualising the retina in great detail and helps in assessing retinal health. However, the structure does not always provide information on the tissue health, and thus techniques which can provide a quantitative, functional aspect of living tissue is required in many cases. The work presented in this thesis aims to develop new devices and techniques which can perform imaging of the retina and to apply them for non-invasive imaging of structure and function in the *in vivo* human retina.

In order to extract structural and functional information from the retina using an SLO, it is essential to understand it's design, construction, and working. For this purpose, **chapter 2** of this thesis discusses the principle of scanning based ophthalmic imaging systems, gives a brief explanation of various design considerations for constructing an SLO, and introduces the retinal oximetry and its importance in diagnosing various retinal diseases. Laser safety considerations for intentional exposure of the retina to the laser light is also described in detail. The knowledge from this chapter forms the basis of the scientific work presented in chapters 3 to 6.

In **Chapter 3**, a novel digital micromirror device (DMD) based SLO is presented. Concentric circle patterns were implemented as a scanning scheme to image the retina and provide fixation at the same time. The DMD was used *in lieu* of traditional scanning mirrors and offered flexibility in terms of speed and confocality. The concentric circles improved the fixation and reduced motion artefacts compared to previously implemented parallel line scanning design. An annulus was used to reduce the corneal reflections from the retina and thereby to increase the signal to noise ratio. *in vivo* imaging was demonstrated by performing non-mydriatic imaging on two subjects at a speed of 7 frames per second with a maximum 20° (diameter) field of view. The images were shot noise limited and clearly show various anatomical features of the retina with high contrast. The images were comparable to images from a commercial SLOs but at a fraction of the cost.

Chapter 4 describes a detailed analysis of the error propagation of measure-

ment noise in retinal oximetry, to identify optimal wavelengths which will yield the lowest uncertainty in saturation estimation for a given measurement noise level. The effect of haemoglobin packing in discrete blood vessels (pigment packing) is also introduced in this chapter. Pigment packing may result in a non-negligible bias in saturation estimation if unaccounted for under specific geometrical conditions, such as sub-diffuse sampling of smaller blood vessels located deeper within the retina. To validate the analysis, an SLO was developed to produce high contrast images. Confocal reflectance measurements were then conducted on a tissue-mimicking scattering phantom with optical properties similar to retinal tissue, including narrow channels filled with absorbing dyes to mimic blood vessels. By imaging at three optimal wavelengths, the 'saturation' of the dye combination was calculated.

In **Chapter 5**, construction of an SLO based on a double-clad fibre coupler and a supercontinuum source is described in detail. Implementation of a balanced detection scheme to suppress the relative intensity noise of the supercontinuum source is also described with experiments validating the improvements in the signal to noise ratio with the use of balanced detection. The optimum wavelengths for accurate *in vivo* oximetry estimation using two wavelengths are established with an *in silico* analysis. The SLO produced dual-wavelength, high-quality images at 10 frames / second with a 20° imaging field of view. The blood oxygen saturation in retinal blood vessels was mapped from the images.

The eye provides a unique location in the human body with visual access to blood vessels. The blood vessels in the eye are regarded as highly superficial and thus is a desirable access point for Hb concentration estimation due to the lack of thick overlying tissues present elsewhere in the body. In **Chapter 6**, a non-invasive spectrophotometric method to image the retina simultaneously at two isosbestic wavelength to extract the haemoglobin concentration values from the two images is described.

Finally, in **Chapter 7**, the discussion on the results obtained from the scientific work in chapters 3-6 is presented with an outlook for future research. The concluding remarks of the thesis are also given in this chapter. This chapter marks the end of the scientific content of the thesis.

References

[1] World Population Ageing: 1950-2050, United Nations Population Division. https://www.un.org/esa/population/publications/worldageing19502050/

[2] R. R. A. Bourne, S. R. Flaxman, T. Braithwaite, M. V. Cicinelli, A. Das, J. B. Jonas, J. Keeffe, J. Kempen, J. Leasher, H. Limburg, K. Naidoo, K. Pesudovs, S. Resnikoff, A. Silvester, G. A. Stevens, N. Tahhan, T. Wong, H. R. Taylor, P. Ackland *et al.* , "Magnitude, temporal trends, and projections of the global prevalence of blindness and distance and near vision impairment: a systematic review and meta-analysis," Lancet Glob. Heal. **5**, (2017).

[3] A. E. Elsner, A. H. Jalkh, and J. J. Weiter, "New devices in retinal imaging and functional evaluation," *Practical Atlas of Retinal Disease and Therapy*, W. Freeman, ed. pp. 19-35, Raven Press, New York (1993).

[4] H. F. Edelhouser, J. L. Ubels, and C. Hejny, "The cornea and the sclera," in Adlers physiology of the eye 10th ed., P. L. Kaufman and A. Alm, eds. (Mosby, Inc., 2003), pp. 47-114.

[5] H. A. Kadkhodaeian, T. Tiraihi, N. Daftarian, H. Ahmadieh, H. Ziaei, and T. Taheri, "Histological and electrophysiological changes in the retinal pigment epithelium after injection of sodium iodate in the orbital venus plexus of pigmented rats," J. Ophthalmic Vis. Res. 11, 7077 (2016).

[6] Text in the public domain —from page 1015 of the 20th edition of Gray's Anatomy (1918).

[7] Text in the public domain —from page 1016 of the 20th edition of Gray's Anatomy (1918).

[8] Text in the public domain —from page 1017 of the 20th edition of Gray's Anatomy (1918).

[9] S. S. Hayreh, "Acute retinal arterial occlusive disorders," Prog. Retin. Eye Res. **30**, 359-394 (2011).

[10] S. Pi, A. Camino, X. Wei, J. Simonett, W. Cepurna, D. Huang, J. C. Morrison, and Y. Jia, "Rodent retinal circulation organization and oxygen metabolism revealed by visible-light optical coherence tomography," **9**, 58515862 (2018).

[11] J. P. Campbell, M. Zhang, T. S. Hwang, S. T. Bailey, D. J. Wilson, Y. Jia, and D. Huang, "Detailed Vascular Anatomy of the Human Retina by Projection-Resolved Optical Coherence Tomography Angiography," Sci. Rep. **7**, 111 (2017).

[12] A. M. Ichsan, L. M. Herawati, A. Vanny, J. Vimala Jaury, H. S. Muhiddin, and Budu, "Central Retinal Artery Occlusion and Partial Ophthalmoplegia Caused by Hyaluronic Acid Injection Filler Cosmetic," Ann. Clin. Lab. Res. **06**, 14 (2018).

[13] R. A. Linsenmeier, "Effects of light and darkness on oxygen distribution and consumption in the cat retina.," J. Gen. Physiol. **88**, 521-42 (1986).

[14] http://www.who.int/blindness/causes/en/

[15] H. A. Quigley, "Glaucoma," Lancet **377**, 1367-1377 (2011).

[16] N. F. Mokwa, T. Ristau, P. A. Keane, B. Kirchhof, S. R. Sadda, and S. Liakopoulos, "Grading of age-related macular degeneration: Comparison between color fundus photography, fluorescein angiography, and spectral domain optical coherence tomography," J. Ophthalmol. 2013, (2013).

[17] J. K. H. Goh, C. Y. Cheung, S. S. Sim, P. C. Tan, G. S. W. Tan, and T. Y. Wong, "Retinal Imaging

Techniques for Diabetic Retinopathy Screening," J. Diabetes Sci. Technol. **10**, 282294 (2016).
[18] Branch retinal artery occlusion "Https://emedicine.medscape.com/article/1223362-overview"
[19] Institute of vision and optics, http://www.ivo.gr/en/patient/glaucoma/glaucoma.html
[20] Retinal diseases simulation, National eye institute, https://nei.nih.gov/health/examples
[21] M. Hammer and D. Schweitzer, "Quantitative reflection spectroscopy at the human ocular fundus," Phys.Med.Biol. **47**, 179-191 (2002).
[22] F. C. Delori and K. P. Pflibsen, "Spectral reflectance of the human ocular fundus," **28**, 1061-1077 (1989).
[23] N. Bosschaart, G. J. Edelman, M. C. G. Aalders, T. G. van Leeuwen, and D. J. Faber, "A literature review and novel theoretical approach on the optical properties of whole blood," Lasers Med. Sci. **29**, 453-479 (2014).
[24] H. L. F. von Helmholtz, Beschreibung eines AugenSpiegels. Berlin, Germany(1851).
[25] W. Jackman, and J. Webster, "Photographing the retina of the living human eye". Photogr News. **23**, 340-341 (1886).
[26] H. Novothy and D. Alvis, "A method of photogrphing fluorescence in circulating blood in the human retina," Circulation **24**, 82-86 (1961).
[27] R. H. Webb, G. W. Hughes, and O. Pomerantzeff, "Flying spot TV ophthalmoscope," Appl. Opt. **19**, 2991-2997 (1980).
[28] R. H. Webb and G. W. Hughes, "Scanning Laser Ophthalmoscope," IEEE Transactions on Biomedical Engineering, vol. BME-**28**, 488-492, (1981).
[29] R. H. Webb, "Manipulating Laser Light for Ophthalmology," IEEE Engineering in Medicine and Biology Magazine **4**, 12-16, (1985).
[30] R. H. Webb, G. W. Hughes, and F. C. Delori, "Confocal scanning laser ophthalmoscope.," Appl. Opt. **26**, 1492-1499 (1987).
[31] F. C. Delori, J. S. Parker, and M. A. Mainster, "Light levels in fundus photography and fluorescein angiography," Vision Res. 20, 10991104 (1980).
[32] D. Huang, E. A. Swanson, C. P. Lin, J. S. Schuman, W. G. Stinson, W. Chang, M. R. Hee, T. Flotte, K. Gregory, C. A. Puliafito, and J. G. Fujimoto, "Optical Coherence Tomography HHS Public Access," Science **22**, 1178-1181 (1991).
[33] A. F. Fercher, K. Mengedoht, and W. Werner, "Eye-length measurement by interferometry with partially coherent light," Opt. Lett. **13**, 186 (1988).
[34] C. K. Hirzenberger, "Optical Measurement of the Axial Eye Length by Laser Doppler Interferometry," Invest. Ophthalmol. **32**, 616624 (1991).
[35] M. Kernt and M. W. Ulbig, "Wide-Field Scanning Laser Ophthalmoscope Imaging and Angiography of Central Retinal Vein Occlusion," Circulation **121**, 14591460 (2010).
[36] L. S. Lim, P. Mitchell, J. M.Seddon, F. G. Holz, T. Y. Wong, "Age-related macular degeneration", Lancet. **379**, 1728-38 (2012).
[37] B. Braaf, K. V. Vienola, C. K. Sheehy, Q. Yang, K. A. Vermeer, P. Tiruveedhula, D. W. Arathorn, A. Roorda, and J. F. de Boer, "Real-time eye motion correction in phase-resolved OCT angiography with tracking SLO," Biomed. Opt. Express **4**, 51 (2013).
[38] K. V. Vienola, M. Damodaran, B. Braaf, K. A. Vermeer, and J. F. De Boer, "In vivo retinal imaging for fixational eye motion detection using a high-speed digital micromirror device (DMD)-based ophthalmoscope," Biomed. Opt. Express **9**, 591602 (2018).
[39] C. K. Sheehy, Q. Yang, D. W. Arathorn, P. Tiruveedhula, J. F. de Boer, and A. Roorda, "High-speed, image-based eye tracking with a scanning laser ophthalmoscope," Biomed. Opt. Express **3**, 2611 (2012).
[40] K. V. Vienola, B. Braaf, C. K. Sheehy, Q. Yang, P. Tiruveedhula, D. W. Arathorn, J. F. de Boer, and A.

Roorda, "Real-time eye motion compensation for OCT imaging with tracking SLO," Biomed. Opt. Express **3**, 2950 (2012).

[41] C. K. S. Leung, A. C. K. Cheng, K. K. L. Chong, S. L. King, S. Mohamed, C. S. L. Lau, C. Y. L. Cheung, G. C. H. Chu, R. Y. K. Lai, C. C. P. Pang, and D. S. C. Lam, "Optic disc measurements in myopia with optical coherence tomography and confocal scanning laser ophthalmoscopy," Investig. Ophthalmol. Vis. Sci. **48**, 3178-3183 (2007).

[42] J. E. DeLeon Ortega, L. M. Sakata, B. Kakati, G. McGwin, B. E. Monheit, S. N. Arthur, and C. A. Girkin, "Effect of glaucomatous damage on the repeatability of confocal scanning laser ophthalmoscope, scanning laser polarimetry, and optical coherence tomography," Investig. Ophthalmol. Vis. Sci. **48**, 1156-1163 (2007).

[43] J. I. W. Morgan and E. N. Pugh, "Scanning laser ophthalmoscope measurement of local fundus reflectance and autofluorescence changes arising from rhodopsin bleaching and regeneration," Investig. Ophthalmol. Vis. Sci. **54**, 2048-2059 (2013).

[44] J. V. Kristjansdottir, S. H. Hardarson, G. H. Halldorsson, R. A. Karlsson, T. S. Eliasdottir, and E. Stefánsson, "Retinal oximetry with a scanning laser ophthalmoscope," Investig. Ophthalmol. Vis. Sci. **55**, 3120-3126 (2014).

[45] B. Zhang, N. Li, J. Kang, Y. He, and X. Chen, "Adaptive optics scanning laser ophthalmoscopy in fundus imaging, a review and update," Int. J. Ophthalmol. **10**, 1751-1758 (2017).

[46] S. Marcos, J. S. Werner, S. A. Burns, SA, W. H. Merigan, P. Artal, D. A. Atchison, K. M. Hampson, R. Legras, L. Lundstrom, G. Yoon, J. Carroll, S. S. Choi, N. Doble, A. M. Dubis, A. Dubra, A. Elsner, R. Jonnal, M. Paques, Y. Zhang, M. Campbell, J. Hunter, A. Metha, G. Palczewska, J. Schallek, and L. C. Sincich, "Vision science and adaptive optics, the state of the field.," Vision Res. **132**, 3-33 (2017).

[47] Y. Kaizu, S. Nakao, I. Wada, M. Yamaguchi, K. Fujiwara, S. Yoshida, T. Hisatomi, Y. Ikeda, T. Hayami, T. Ishibashi, and K. Sonoda, "Imaging of Retinal Vascular Layers: Adaptive Optics Scanning Laser Ophthalmoscopy Versus Optical Coherence Tomography Angiography," Transl. Vis. Sci. Technol. **6**, 2 (2017).

[48] W. Drexler and J. G. Fujimoto, "State-of-the-art retinal optical coherence tomography," Prog. Retin. Eye Res. **27**, 45-88 (2008).

[49] A. G. Podoleanu and R. B. Rosen, "Combinations of techniques in imaging the retina with high resolution," Prog. Retin. Eye Res. **27**, 464499 (2008).

[50] A. G. Podoleanu, "Optical coherence tomography," J. Microsc. **247**, 209-219 (2012).

[51] S. H. Yun, G. J. Tearney, B. E. Bouma, B. H. Park, and J. F. De Boer, "High-speed spectral-domain optical coherence tomography at 1.3 μm wavelength," Opt. Express **11**, 35983604 (2003).

[52] T. C. Chen, A. Zeng, W. Sun, M. Mujat, and J. F. De Boer, "Spectral-domain optical coherence tomography and glaucoma," Int. Ophthalmol. Clin. **48**, 2945 (2008).

[53] J. F. de Boer, B. Cense, B. H. Park, M. C. Pierce, G. J. Tearney, and B. E. Bouma, "Improved signal-to-noise ratio in spectral-domain compared with time-domain optical coherence tomography," Opt. Lett. **28**, 2067 (2003).